A Ioffe Trap Magnet for the Project 8 Atom Trapping Demonstrator

Alexey L. Radovinsky, Alec Lindman, *Member, IEEE*, Joseph A. Formaggio, and Joseph V. Minervini, *Senior Member, IEEE*

***Abstract*—The goal of the Project 8 experiment (B. Monreal and J. Formaggio, 2009) is to measure the absolute neutrino mass using tritium, which involves precisely measuring the energies of the beta-decay electrons in the high-energy tail of the spectrum (A. A. Esfahani *et al.*, 2017). The experimental installation of Project 8 Atom Trapping Demonstrator requires a magnet with rather unusual field properties. The magnet has to contain within the cold mass a large volume enclosed by a continuous, uninterrupted boundary higher than 2 T, whereas the field in a substantial volume inside this boundary has to be of the order of 10^{-4} T or less. A 1-T solenoid field provides the background field necessary for the detection of the beta-decay electrons (A. A. Esfahani *et al.*, 2019). A proposed toroidal magnet system [a Ioffe-Pritchard trap (T. Bergeman *et al.*, 1987)] comprised of specially shaped multiple racetrack windings with opposing polarities satisfies these unusual requirements. The magnet is made of NbTi wire and expected to be conduction cooled. Manufacturability issues are addressed as well as the effect of tolerances on the field quality. The design includes additional topological features providing a low-field duct for interfacing with the peripheral coils of the velocity and state selector.**

***Index Terms*—Superconducting magnets, neutrino sources, atomic measurements, atom optics, particle beam injection.**

I. Introduction

THE proposed Atom Trapping Demonstrator (ATD) magnet system is composed of a trap magnet, an MRI-type background solenoid, and coils to interface with peripheral coils in the Velocity and State Selector (VSS), which supplies cold atoms to the trap. The coils defined in this study define the ATD at a conceptual level; the resulting parameters will inform a preliminary cost estimate.

The atom trap must confine tritium atoms in a magnetic bottle at 10^{12} cm^{-3} [2]; a reasonable temperature (30–50 mK) implies a trap depth of 2 T. We have generalized the widely-used quadrupole Ioffe [4] trap to higher multipole order and dramatically reduced the size of the pinch coils. This opens the path towards a trap of ten-plus cubic meters as required for Phase IV of Project 8 [2]. The proposed ATD design uses well-established NbTi superconductor to provide a magnetic field shape that traps the tritium atoms, is nominally compatible with the requirements on the magnetic field in the fiducial volume, and that accommodates the antennae that collect the CRES signals. See Section VII for the detailed constraints.

Manuscript received September 24, 2019; accepted March 13, 2020. Date of publication April 6, 2020; date of current version May 1, 2020. This work was supported in part by the US DOE Office of Nuclear Physics, in part by the National Science Foundation under Award 1205100 and 1505678 to MIT, in part by the PRISMA+ Cluster of Excellence (EXC2118/1) at JGU Mainz, and in part by internal investments at all institutions. *(Corresponding author: Alexey Radovinsky.)*

Alexey L. Radovinsky is with the Plasma Science and Fusion Center, Massachusetts Institute of Technology, Cambridge, MA 02139 USA (e-mail: radovinsky@psfc.mit.edu).

Alec Lindman is with PRISMA + Cluster of Excellence Institut für Physik, Johannes-Gutenberg Universität 55122 Mainz, Germany.

Joseph A. Formaggio is with Department of Physics, Massachusetts Institute of Technology, Cambridge, MA 02139 USA (e-mail: josephf@mit.edu).

Joseph V. Minervini is with Plasma Science and Fusion Center, Massachusetts Institute of Technology, Cambridge, MA 02139 USA (e-mail: minervin@mit.edu).

Color versions of one or more of the figures in this article are available online at https://ieeexplore.ieee.org.

Digital Object Identifier 10.1109/TASC.2020.2985675

II. Coil Composition

Fig. 1 depicts general layout of the coils of the Trap Magnet. It is comprised of 8 short (hereinafter referred to as Coil A) and 4 long (Coil B) racetracks, assembled in a toroidal configuration. Polarities of the racetrack dipoles alternate circumferentially. Each coil is expected to be embedded into an individual mandrel forming 12 subassemblies, later integrated into the cold mass assembly by means of intermediate structural links. The detailed design will be developed later.

III. General Parameters

The magnetic design of the windings is defined by a Dassault Systems Opera COND file, which will be submitted to a manufacturer. The racetrack coils are expected to be wound using insulated NbTi wire; windings will be integrated with aluminum mandrels by means of epoxy impregnation. The coils are to be electrically connected in series and the baseline plan is to conductively cool them with cryocoolers.

There is a possibility that the Project will require operating the windings at a low temperature, perhaps 1–3 K, to achieve sufficient projection of the trapping contour from the winding face. In that case additional modifications of the cryogenic system will be required. One option is to provide a forced flow of subcooled helium in a tube thermally connected to the aluminum coil mandrel.

Table I shows general parameters characterizing the magnet: peak field on the conductor, $B_{\max}$, stored electromagnetic energy, E, total volume, length and outer diameter of the windings, $V_{\rm m}$, $L_{\rm m}$ and $D_{\rm m}$; wire: area and diameter of insulated and bare wire, as well as thickness of insulation and copper-to-superconductor ratio CU/SC; characteristics of the winding: fill factor $f_{\rm fill}$, thickness, height and area of rectangular cross section of the winding, T, H and $A_{\rm w}$, number of turns per coil, $N_{\rm turns}$, and total length of the wire in all coils, $l_{\rm total}$; engineering current density, J, operating current, $I_{\rm op}$, critical current (conservatively chosen at 5 T and 5 K), fraction of critical $f_{\rm c}$, and finally total inductance of the magnet, L.

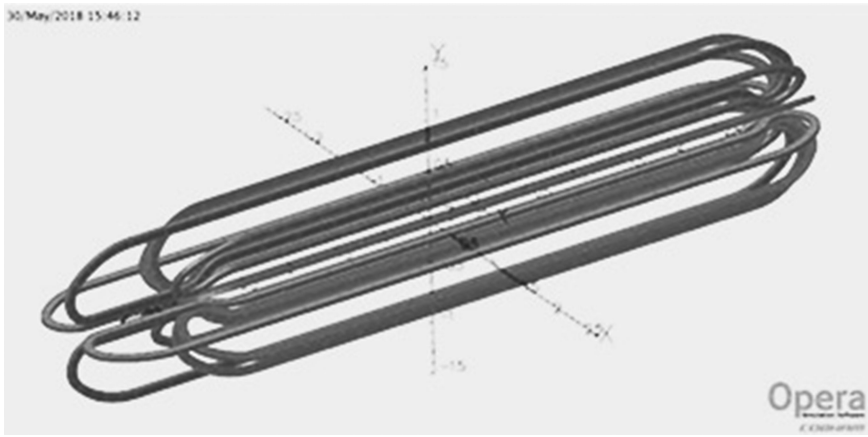

Fig. 1. The proposed trap magnet is composed of 12 racetrack coils with opposing polarities.

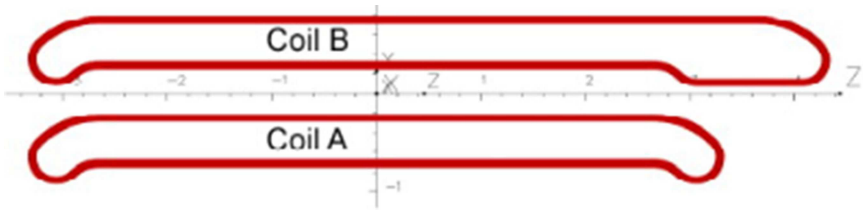

Fig. 2. The "Coil A" and "Coil B" racetracks shapes as used in the trap magnet.

TABLE I
SELECTED PARAMETERS OF THE PROPOSED TRAP MAGNET

Magnet	B_{max} (T)	4.69	Current	J (A/mm^2)	200
	E (MJ)	12.32		Iop (A)	387
	V_m (m^3)	0.558		I_c at 5 T and 5 K	600
	L_m (m)	7.6		f_c	0.64
	D_m (m)	0.8		L (H)	164.54
Wire	A_{ins} (mm^2)	1.683	Winding	f_{fill}	0.87
	D_{ins} (mm)	1.464		T (mm)	80
	T_{ins} (mm)	0.035		W (mm)	40
	D_{bare} (mm)	1.394		A_w (mm^2)	3200
	A_{bare}	1.562		N_{turns}	1654
	CU/SC	3:1		l (km)	288

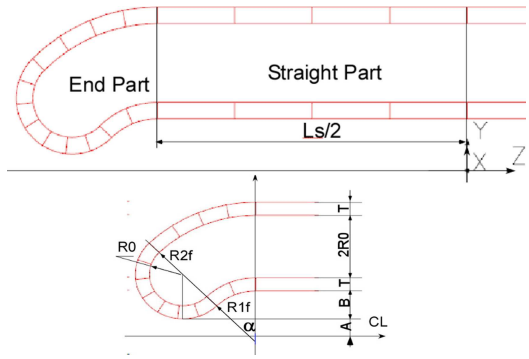

Fig. 3. Key dimensions of a Coil A racetrack, including their relation to the global coordinate system. See the text for their proposed values.

IV. MANUFACTURABILITY

The trap magnet is comprised of 12 racetrack-shaped windings. As shown in Fig. 2, the racetrack coils have both positive (outward) and negative (inward) curvature. We have developed a method, to be discussed elsewhere, to wind these coils using standard equipment designed for winding positive-curvature coils.

Fig. 3 show the composition and the dimensions of the coil. It is comprised of a Straight Part made of straight legs and of two End Parts, each made of three constant-radius arcs.

The following dimensions are used in the present design: $L_s = 5.30$ m, $A = 0.08$ m, $B = 0.17$ m, $T = 0.08$ m, $R_0 = 0.19$ m, $\alpha = 45$ deg. The rectangular cross section of the winding is $H = 0.04$ m thick. The remaining, radial dimensions are derived from the given dimensions. Measured from the vertical axis these radii are

$$R_1^f = B/\left(1-\cos\left(\alpha\right)\right) - R_0 - T = 0.310 \text{ m and}$$

$$R_2^f = R_1^f + T + 2R_0 = 0.770 \text{ m}.$$

Here the superscript "f" indicates the final shape of the magnet.

V. DIFFERENCES BETWEEN COILS A AND B

The difference between Coils A and B is that in Coil B one of the ends is modified to make it longer as shown in Fig. 2.

Fig. 4 illustrates conversion of the end of Coil A to form the end of Coil B. It is done by adding two pairs of straight segments marked in Fig. 4 by letters *a* and *b*. In this model, 1-m long segments *a* extend the end curve of Coil B making it longer. Short 1.4-cm-long segments *b* move the leg closest to the axis 1 cm closer to the axis, slightly reducing the aperture of the coil

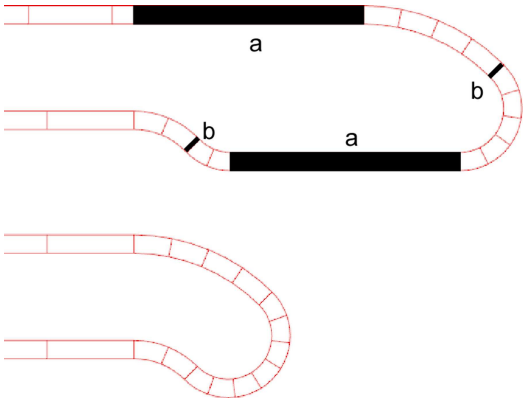

Fig. 4. The end of a Coil B racetrack.

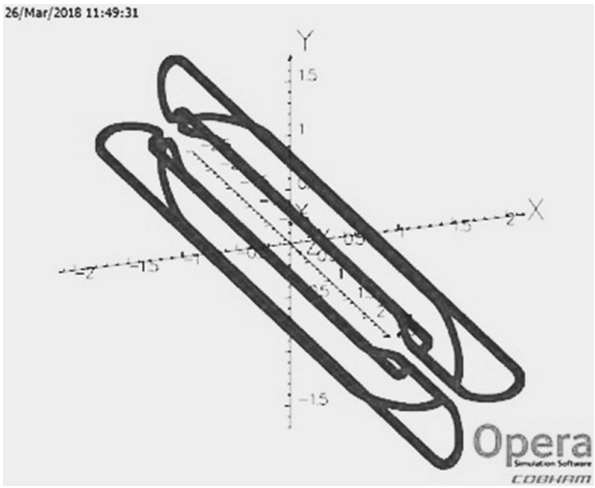

Fig. 5. The basic quadrupole of the trap magnet, formed from B Coils.

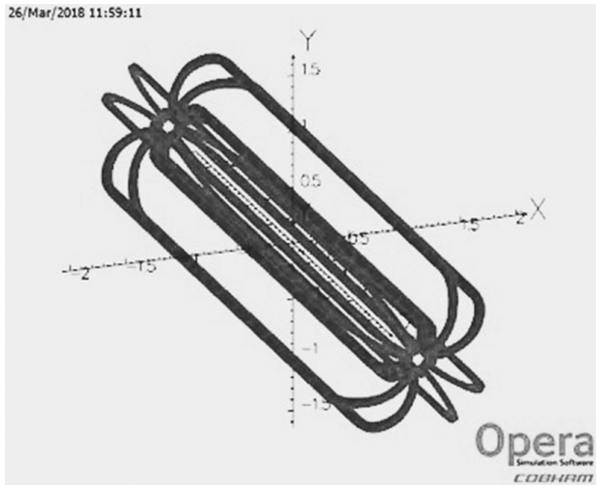

Fig. 6. The intermediate A Coils located between the basic quadrupole coils.

TABLE II
FORCES IN THE PROPOSED TRAP MAGNET

Coil/Type	θ (°)	F_x	F_y	F_r	F_z
1/B	0	169	0	169	10
2/A	30	127	56	138	-5
3/A	60	56	127	138	-5
4/B	90	0	169	169	10
5/A	120	-56	127	138	-5
6/A	150	-127	56	138	-5
7/B	180	-169	0	169	10
8/A	210	-127	-56	138	-5
9/A	240	-56	-127	138	-5
10/B	270	0	-169	169	10
11/A	300	56	-127	138	-5
12/A	330	127	-56	138	-5
Sum		0	0	1779	0

assembly. The latter facilitates continuity of the 2-T boundary in this area.

The purpose of extended-length quadrupole formed by Coils B is to provide a continuous high-field boundary in the transition between the Trap Magnet and the coils of the VSS magnet. Details of this transition are beyond the scope of this paper.

The following illustrations show how Coils A and B combine to form the trap magnet. First, we take four Coil Bs and arrange them in a quadrupole (with alternating polarities), as shown in Fig. 5. Next, we take eight Coil As, arranged as shown in Fig. 6 and add them to those in Fig. 5; together they form the arrangement shown in Fig. 1. Coil polarities alternate. This completes the assembly of the proposed trap magnet.

VI. FORCES

Detailed design of the Cold Mass (CM) support structure will be developed later. Here we address only the general pattern and magnitude of forces in this rather unconventional magnet.

First, note that all electromagnetic (EM) forces are self-contained in the CM and fringe fields are extremely low; thus, there will be no EM loads on the cold-to-warm supports of the CM in the cryostat. Note that due to the magnetically decoupled nature of interaction between toroidal and poloidal magnets, this is true even when the Trap Magnet operates within the Background Solenoid, independently whether the Trap Magnet and the Background Solenoid are in the same or in separate cryostats.

There will be internal interaction forces between the racetracks within the CM. Due to the fact that the racetracks are assembled in a torus with alternating polarities, the dominant forces will be from repulsion between the coils. This will c create a radial net force on individual racetracks. The CM structure must contain these forces.

Table II summarizes forces on individual coils, numbered as shown in Fig. 7. Here θ is the angle between the *X*-*Z* plane and the mid-plane of the respective racetrack. Force components in metric tons of force are shown in the Cartesian coordinates, alongside the radial component F_{r}.

Note that axial forces F_z are generally much smaller than the radial forces. All radial forces are positive, tending to expand the magnet radially. The difference between radial forces on individual coils is because coils 1, 4, 7, and 10, are of type B and are longer than the rest of the coils; the remainder are of the shorter A type. The following considerations help in assessing the scale of these forces. Assume that the radial forces are restrained by a cylindrical structure, surrounding the assembly shown in Fig. 1. Let us assume that this cylinder is $L = 5$ m long, has radius $R = 0.8$ m and thickness $T = 1.25$ cm.

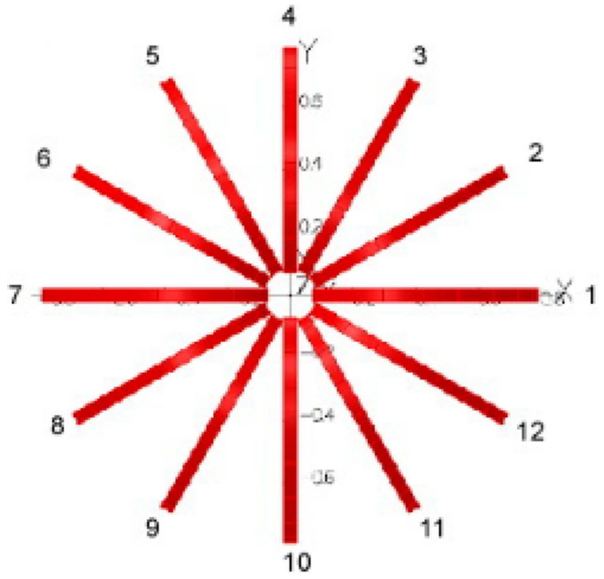

Fig. 7. The numbering of the coils.

The average radial pressure from the radial coil forces is then

$$p = \Sigma F_{\mathrm{r}} / (2\pi RL) = 0.69\ \mathrm{MN/m^2}.$$

This translates into the averaged hoop stress in the support cylinder, $S_{hoop} = pR/T = 44$ MPa, which is about one-quarter of the allowable tensile stress for alloy-6061 aluminum, a traditional material for cold mass structures. We conclude that the stresses in the cold mass structure are not expected to be challenging.

VII. Field Requirements and Tolerances

There are two major field requirements applied to the magnetic field distribution and quality of this magnet. The first requirement is to provide some nonzero space between the inner face of the winding and the 2-T field surface. This permits installation of several components: the racetrack support structure, multiple thermal shields at various temperatures to isolate the magnet windings from the central experimental volume, and the all-important antennae which collect the CRES signals.

The thermal isolation is the most significant driver of the requirement on the gap between the windings and the trapping isosurface, since the inner wall of the experimental space needs to operate between 2 K and 90 K while the trap magnet coils remain below 5 K. We have examined the field of the proposed trap magnet in three dimensions and found a nonzero gap everywhere. Once the required size of the gap is determined, we will assess whether the present gap is sufficient.

Here we use another approach to assess the same issue, this time using a finite element model in Opera. Besides its similarity to the Biot-Savart-based contour plotting, like that shown in Fig. 8 for the axial cross section at $Z = 0$, this model can generate field maps on boundaries between materials, where the field may be limited by some particular constraint. Fig. 9 shows a field map on the boundary of the windings at one of the ends of the magnet, where the field B is higher than 2 T. The pattern of the mapped space forms a trough with a solid, uninterrupted barrier around the void hosting the winding. Other parts of the magnet

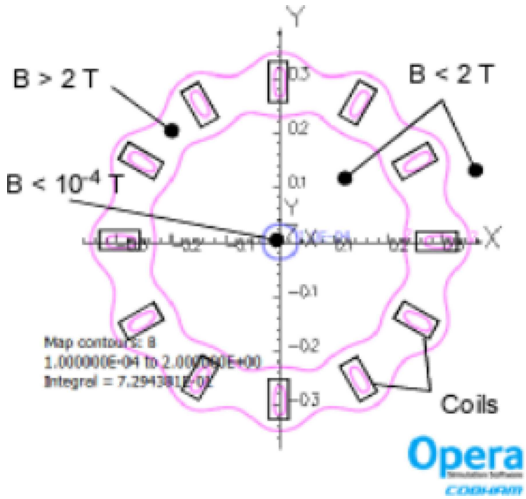

Fig. 8. The 2-T and 10^{-4}-T boundaries in the transverse plane at z = 0.

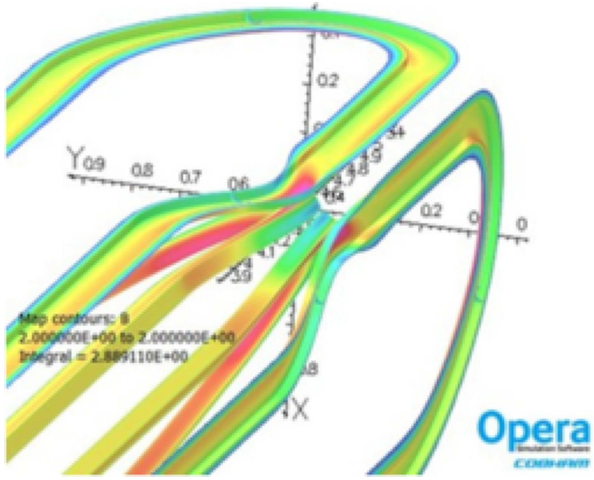

Fig. 9. Regions of B > 2 T around the coils.

were examined visually and proved the continuity of the 2-T boundary layer around the winding.

The second requirement on the field quality is that the field in some volume within the magnet shall be very small. The cross-sectional contour map in Fig. 8 shows the circular area with $B < 10^{-4}$ T in the central part of the $Z = 0$ cross section. These are theoretical patterns calculated using an ideal coil build with zero deviations from the nominal shapes and positions.

The real magnet will differ from the "ideal" model in many ways. At this time there is no practical way of assessing all these possible deviations. However, one simple way of modeling the impact of deviations on the field quality is to "distort" it by applying small displacements to one coil in the assembly.

Results show that this deviation leaves practically no space with $B < 10^{-4}$ T; small, broken-up spaces with $B < 10^{-3}$ T; and larger spaces with $B < (1.5 - 2.0) \times 10^{-3}$ T. This exercise shows that maintaining adequate tolerances in the process of manufacturing this rather large and complex magnet may be challenging. In the later iterations of the design, we will calculate the maximum allowable geometric tolerances consistent with maintaining the required magnetic field in the trapping volume.

VIII. Summary

This preliminary design for a large-volume atomic tritium trap makes use of Ioffe-Pritchard coils and existing superconducting magnet technology to meet the challenging magnetic requirements of the Project 8 experiment. Construction of the Atom Trapping Demonstrator will verify the trapping performance and manufacturability of a cubic-meter-scale atomic tritium trap. Future work will assess the mechanical tolerances and cryogenic strategies needed to meet the specifications imposed by Project 8's physics goals.

References

[1] B. Monreal and J. Formaggio, "Relativistic cyclotron radiation detection of tritium decay electrons as a new technique for measuring the neutrino mass," *Phys. Rev. D*, vol. 80, Sep. 9, 2009, Art. no. 051301(R).

[2] A. A. Esfahani *et al.*, "Determining the neutrino mass with cyclotron radiation emission spectroscopy — Project 8," *J. Phys. G: Nucl. Part. Phys.*, vol. 44, 2017, Art. no. 054004.

[3] A. A. Esfahani *et al.*., "Electron radiated power in cyclotron radiation emission spectroscopy experiments," *Phys. Rev. C*, vol. 99, May 2, 2019, Art. no. 055501.

[4] T. Bergeman, G. Erez, and H. J. Metcalf, "Magnetostatic trapping fields for neutral atoms," *Phys. Rev. A*, vol. 35, no. 4, 1987, Art. no. 1535.